Multi-objective optimization of a wave energy absorber geometry

Adi Kurniawan **Torgeir Moan**
adi.kurniawan@ntnu.no torgeir.moan@ntnu.no
Centre for Ships and Ocean Structures, Trondheim, Norway

1 Introduction

In terms of power performance, it is desirable for a wave energy absorber to have not only high levels of power absorption but also a broad absorption bandwidth. However, it may be the case that superior power performance is achieved at the expense of a high structural cost. Therefore, apart from maximizing the power absorption, we also need to minimize the cost of the absorber. The two objectives are, in general, conflicting, and it is not obvious what constitutes the best trade-off solution. In this study we pose this problem as a multi-objective optimization problem. An optimization algorithm is used to optimize the geometry of a wave energy absorber, with the objectives of maximizing the maximum mean absorbed power and minimizing the surface area of the absorber. The latter is supposed to be indicative of the structural cost.

2 Formulation of the problem

Consider a wave energy absorber which oscillates in one degree of freedom in response to incident regular plane waves of angular frequency ω. We assume that the power take-off is effected by a linear damper with coefficient R_u. Let M be the inertia of the absorber, m the added inertia, R the radiation damping coefficient, and S the restoring coefficient. The absorber velocity U and the wave exciting force X_e are related through the equation of motion of the absorber:

$$X_e = (R_u + Z)\,U, \tag{1}$$

where $Z = R + \mathrm{i}\omega\left(M + m - S\omega^{-2}\right)$. The maximum mean power that can be absorbed by the linear damper is given as

$$P_{\max} = \frac{|X_e|^2}{4(R + |Z|)}, \tag{2}$$

obtained when $R_u = |Z|$. On the other hand, the maximum theoretical limit of achievable mean power is

$$P_{\lim} = \frac{|X_e|^2}{8R}. \tag{3}$$

Comparing (2) and (3), we see that $P_{\max} = P_{\lim}$ when

$$M + m - S\omega^{-2} = 0. \tag{4}$$

In this case the velocity U is in phase with the exciting force X_e, and the system is at resonance. When (4) is not satisfied, $P_{\max} < P_{\lim}$. Multiple resonances (Evans and Porter, 2012) are achieved if (4) is satisfied for more than one frequency. If it is possible to have these frequencies lie within the range of typical wave frequencies occurring at sea, we have a good wave energy absorber in terms of its power performance.

To have a cost-effective wave energy absorber, however, we also need to minimize its cost. A number of cost indicators may be identified for a wave energy absorber (see, e.g. Babarit et al., 2012), but for simplicity, in this study we consider only one cost indicator, namely the surface area A_s. Thus $P_{\max}$ is to be maximized for a given range of frequencies while A_s is to be minimized. This is a multi-objective optimization problem with two objectives. Since the objectives are, in general, conflicting, instead of a single optimum, there are multiple optimum solutions. The task is to identify these optimum solutions.

The problem can be formulated as follows: for $V_{\min} \le V \le V_{\max}$, where V is a set of geometric variables, find V which maximize $f_1^{\mathrm{obj}}(V) = \int_{\omega_{\min}}^{\omega_{\max}} P_{\max}(\omega)\,\mathrm{d}\omega$ and minimize $f_2^{\mathrm{obj}}(V) = A_s$. Here, $\omega_{\min}$ and $\omega_{\max}$ are the specified minimum and maximum frequencies.

3 Methodology

A multi-objective optimization algorithm is used to solve the above problem. The algorithm works by generating successive (random) *populations* through *selection* and *variation* operations. A population is defined as a collection of *individuals*, where an individual is a set of design variables. Selection consists of retaining the 'best' individuals in the population and ensuring the spread of these individuals. The 'best' set of individuals are identified from the population by sorting their objective function values such that in this set there is no individual which improves an objective without worsening another one. The spread of individuals is ensured by grouping individuals with objective function values close to each other, retaining just one individual in this group, and discarding the rest. Variation consists of generating new individuals to be added to the set of individuals which survive the selec-

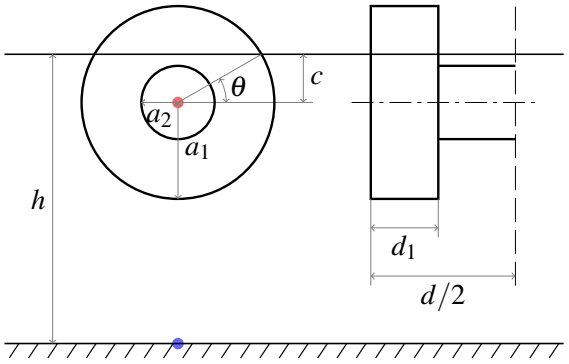

Figure 1: Two-dimensional sketch (side and front views).

tion process, to make up a new population. The new population is again subjected to selection and variation operations, and the process is repeated for a number of *generations*, or iterations, until convergence is observed. The final population is taken as the optimum set of solutions.

For each individual, $P_{\max}$ is obtained according to (2), where the hydrodynamic parameters X_e, m, and R are computed using the higher-order panel method of WAMIT, whereas A_s is calculated from known formulas. Here, A_s is taken as the total surface area and not the submerged surface area. The whole optimization routine is programmed in MATLAB, which then needs to perform repeated calls of WAMIT. The basic geometry is modelled using MultiSurf, and by virtue of the link between WAMIT and the Relational Geometry Kernel of MultiSurf (Lee et al., 2002), any variations in dimensions may be imposed only by modifying a few lines in the Geometric Data File. Further, it is convenient to minimize both objective functions instead of maximizing one and minimizing the other. Thus, the first objective function is recast into $f_1^{\text{obj}} = k/\int_{\omega_{\min}}^{\omega_{\max}} P_{\max}(\omega)\,\mathrm{d}\omega$, where k is a scale factor which is used so that the values of f_1^{obj} is comparable to those of f_2^{obj}.

4 Case study

We consider a wave energy absorber in the form of a horizontal composite circular cylinder oscillating about a horizontal axis fixed at the bottom, where the power take-off is located. The geometry of the cylinder consists of a central part and two surface-piercing ends. The central part, which is submerged close to the water surface, has the purpose of introducing multiple resonances. The two ends, which are of a larger diameter, have the purpose of supplying additional buoyancy. A sketch of the cylinder is shown in Fig. 1.

Table 1: Variables of the cylinder

Geometric variable	min [m]	max [m]
Total width (d)	4	20
Thickness of larger cylinders (d_1)	1	$d/2-1$
Radius of larger cylinders (a_1)	2	7
Radius of smaller cylinder (a_2)	1	$0.95c$

The variables to be optimized are the radii of the larger cylinders and the smaller cylinder, a_1 and a_2, as well as the thickness of the larger cylinders d_1 and the total width d (see Table 1 for the specified limits). The ratio of the depth of submergence of the cylinder axis c to the radius of the larger cylinder a_1 is fixed. For this geometric configuration, $S = (M_w - M)g(h - c) + 4\rho g d_1 a_1^3 \cos^3\theta/3$, where M_w is the mass of the displaced water and h is the water depth.

Results are obtained for $h = 15$ m, incident wave amplitude $A = 1$ m, $c/a_1 = 0.6$, $M/M_w = 0.4$, $\omega_{\min} = 0.4$ rad/s, and $\omega_{\max} = 1.3$ rad/s. The hydrodynamic parameters are computed for every 0.02 rad/s. Interpolation is used to refine this resolution by a factor of 3. A population size of 10 is chosen, and the maximum number of generations is 4. The total time taken to complete the optimization in this case was less than 3 hours on a 2.50 GHz, 2.96 GB RAM PC.

The evolution of the 'best' solutions at the end of each generation is shown in Fig. 2 (top). The optimum geometries at the end of generation 4 are shown in Fig. 3, and the corresponding objective function values are plotted in Fig. 2 (middle). It is clear that among the optimum geometries, more power can be absorbed only by increasing the surface area. Further, it is observed that the radii of the central cylinder tend to the maximum limit. This could be explained by the fact that more energy is available close to the water surface. On the other hand, the radii of the larger cylinders are not maximized. In fact, for geometries 6 to 10, $a_1 = 2$ m, the minimum limit.

The maximum mean absorbed power is plotted in Fig. 4 (right) for some selected optimum geometries, while Fig. 4 (left) shows the behaviour of the added inertia and the function $S\omega^{-2} - M$. It is shown that the frequencies for which the added inertia intersects the function $S\omega^{-2} - M$ correspond to the frequencies where $P_{\max} = P_{\lim}$. A case of multiple resonances is seen for geometry 1.

The next step after identifying the set of optimum solutions is to choose one solution from it. Further information is required for this purpose, but for the present, let us say that the optimum should minimize the ratio of A_s to $\int_{\omega_{\min}}^{\omega_{\max}} P_{\max}(\omega)\,\mathrm{d}\omega$. Then, according to Fig. 2 (bottom), geometry 6 should be chosen.

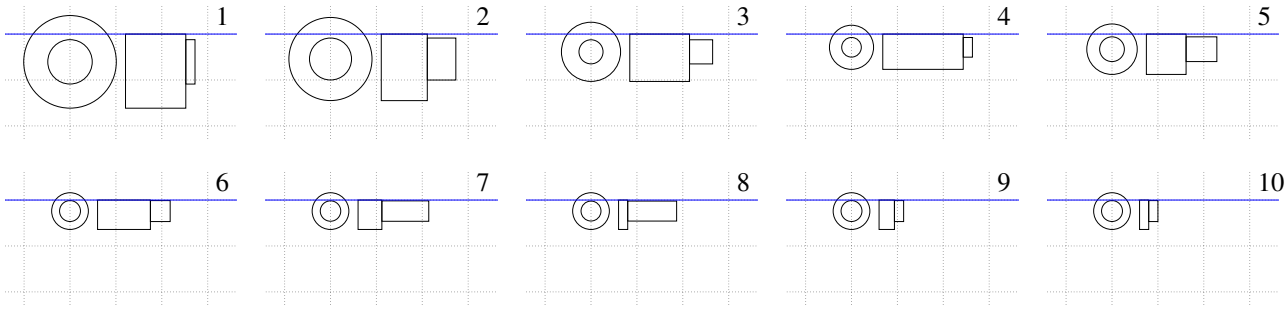

Figure 3: Optimum geometries. One grid is 5×5 m^2.

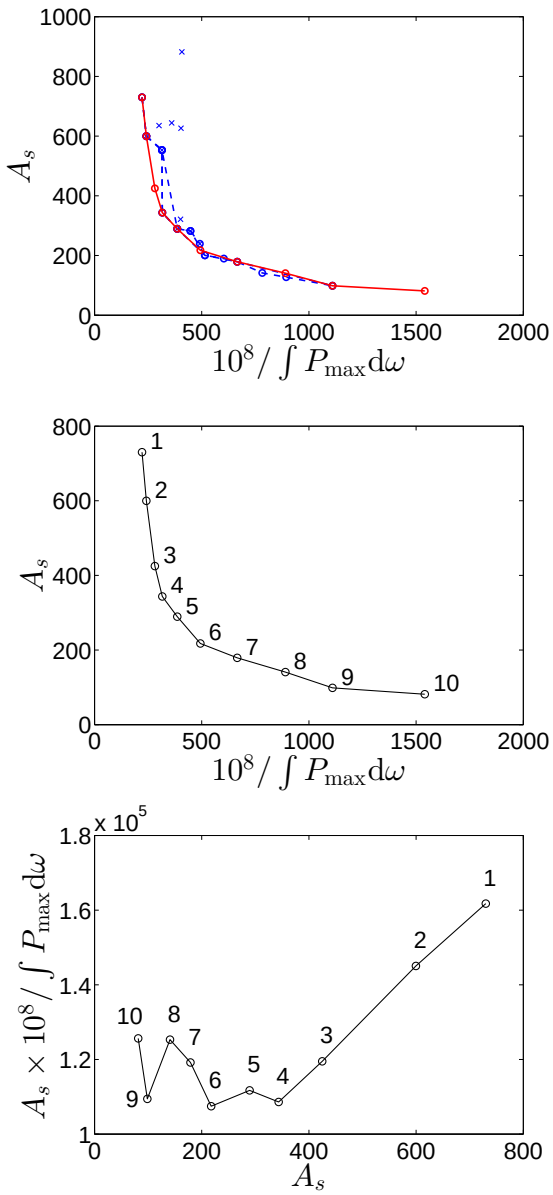

Figure 2: Top: Initial population (crosses) and 'best' solutions at the end of each generation (circles), plotted in the objective function space. The final solutions are identified in red. Middle: Final objective function values. Bottom: f_2^{obj} versus $f_1^{\text{obj}} f_2^{\text{obj}}$.

5 Conclusion

The increasing efficiency of today's computers has permitted intensive numerical optimizations to be carried out within a reasonable time. We have illustrated this by presenting an example of how a multi-objective optimization algorithm may be used to optimize the geometry of a wave energy absorber in the form of a composite circular cylinder. While we have used simple expressions as the optimization objectives in this example, the importance of considering other objectives besides maximizing power absorption is evident.

The present formulation of the problem appears to favour smaller geometries over larger ones. This, however, is likely to be dependent on the selected range of wave frequencies. Further information such as the wave climate, if available, should preferably be included, and more than two objectives may be considered.

The method may be applied to optimize other geometric configurations. It may be worthwhile to compare the present results to those of a uniform circular cylinder. Perhaps more interestingly, the method may be applied to find optimum configurations of arrays of wave energy absorbers, which are not quite practical to study experimentally.

References

A. Babarit, J. Hals, M. J. Muliawan, A. Kurniawan, T. Moan, and J. Krokstad. Numerical benchmarking study of a selection of wave energy converters. *Renewable Energy*, 41(0):44–63, 2012.

D. V. Evans and R. Porter. Wave energy extraction by coupled resonant absorbers. *Phil. Trans. R. Soc. A*, 370(1959):315–344, 2012.

C.-H. Lee, J. S. Letcher Jr., R. G. Mack II, J. N. Newman, D. M. Shook, and E. Stanley. Integration of geometry definition and wave analysis software. In *Proc. 21st Int. Conf. Offshore Mech. Arctic Eng.*, pages 721–733, Oslo, Norway, 2002.

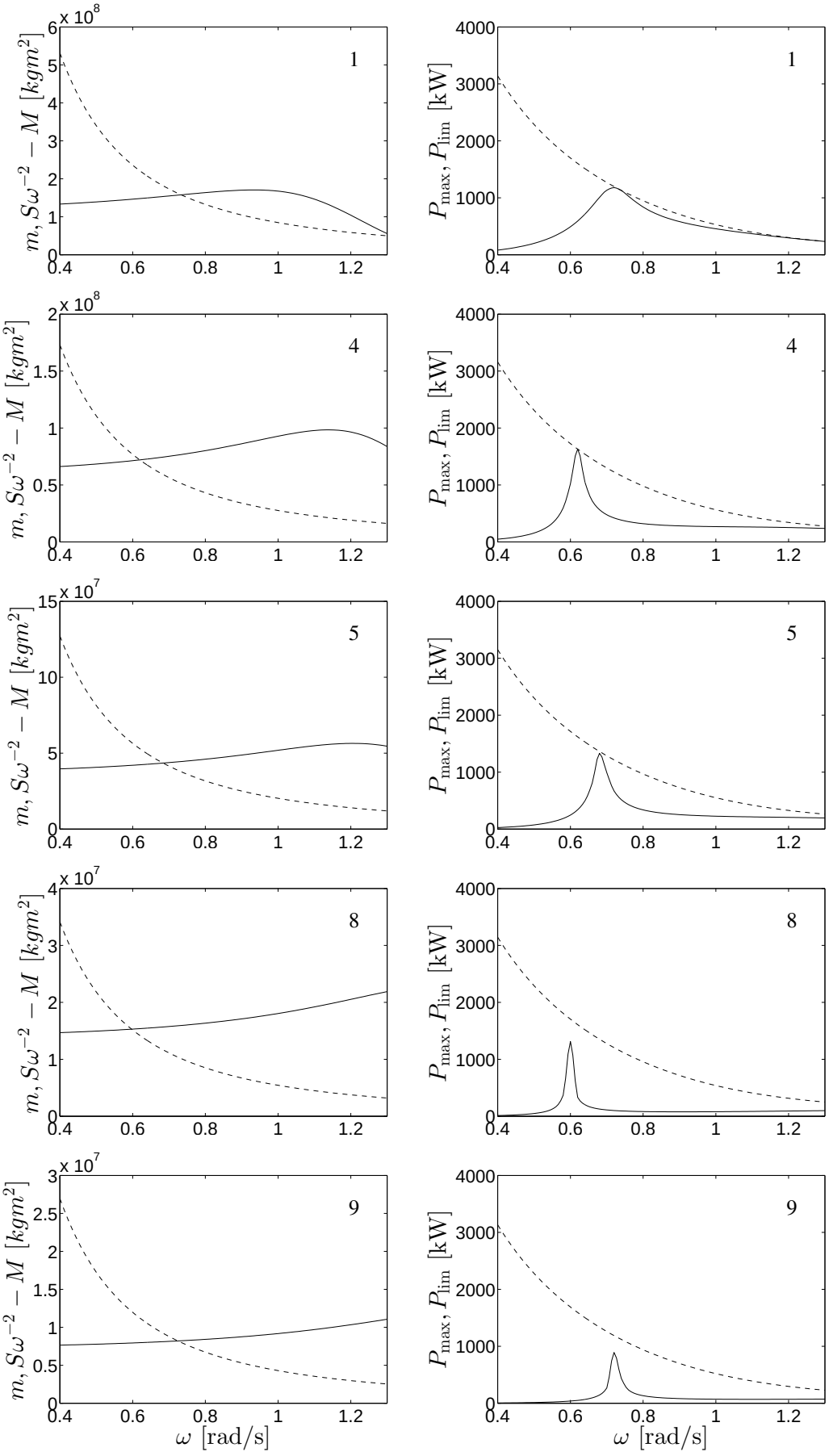

Figure 4: Added inertia and $S\omega^{-2} - M$ (left), and maximum mean absorbed power and the theoretical limit (right), corresponding to optimum geometries 1, 4, 5, 8, and 9.